Advanced Robotics

ISSN: (Print) (Online) Journal homepage: https://www.tandfonline.com/loi/tadr20

A kinematic model generates non-circular human proxemics zones

Fanta Camara & Charles Fox

To cite this article: Fanta Camara & Charles Fox (06 Oct 2023): A kinematic model generates non-circular human proxemics zones, Advanced Robotics, DOI: 10.1080/01691864.2023.2263062

To link to this article: https://doi.org/10.1080/01691864.2023.2263062

Published online: 06 Oct 2023.

ADVANCED ROBOTICS
https://doi.org/10.1080/01691864.2023.2263062

FULL PAPER

OPEN ACCESS Check for updates

A kinematic model generates non-circular human proxemics zones

Fanta Camara[a,b,c] and Charles Fox[b,c]

[a]Institute for Safe Autonomy, University of York, York, UK; [b]Institute for Transport Studies, University of Leeds, Leeds, UK; [c]Lincoln Centre for Autonomous Systems, University of Lincoln, Lincoln, UK

ABSTRACT

Hall's theory of proxemics established distinct spatial zones around humans where they experience comfort or discomfort when interacting with others. Our previous work proposed a new model of proxemics and trust and it showed how to generate proxemics zone sizes using simple equations from human kinematic behaviour. But like most work, this assumed that the zones are circular. In this paper, we refine this model to take the initial heading of the agent into account and find that this results in a non-circular outer boundary of the social zone. These new analytical results from a generative model form a step towards more advanced quantitative proxemics in dual agents' interaction modelling.

ARTICLE HISTORY

Received 20 May 2023
Revised 24 July 2023
and 31 August 2023
Accepted 3 September 2023

KEYWORDS

Proxemics zone shapes; trust; dual agents' behaviour; human–robot interaction

1. Introduction

The increasing prevalence of autonomous robots that operate in human environments has created new challenges in human–robot interaction (HRI). One of the key questions in HRI is how autonomous robots can share and negotiate space with humans, especially in densely populated areas. While robots are typically programmed to be safe and always yield to humans to avoid collisions, this can lead to the 'Freezing robot problem' [1], where the robot may yield indefinitely to a stream of humans, never making progress to its destination.

This problem has motivated the development of game-theoretic models, such as the sequential chicken model [2], which allow for frequent successful interactions by planning for a small but nonzero probability of collision based on the agents' estimates of the probability and utility of a collision versus the value of time lost by yielding. Collisions are not usually actualised, but their possibility creates a 'credible threat' which affects the behaviour of the agents during interactions, encouraging them to negotiate and succeed in these interactions most of the time. Deliberately engineering collision events with a small probability is clearly undesirable. But the sequential chicken model goes on to show that rare severe collisions could be replaced by more frequent but lower severity penalties, if suitable forms of penalty could be found.

Humans are known to have personal spaces [3] and to feel uncomfortable if certain of these spaces are occupied without their consent. It has been proposed in [4] that the invasion of this personal space can be used as a penalty for autonomous robots in the sequential chicken model to avoid collisions. The invasion of personal space can be quantitatively modelled using proxemics, which studies the empirical results on zone sizes and utilities. By combining the chicken model and proxemics, the robot can plan its movements to avoid collisions but occasionally causing them mild discomfort by invading their space. This would enable successful interactions without the risk of physical harm.

The *Personal zone* is the region surrounding a human to a radius of 1.2 m. Humans generally reserve this zone for friends and acquaintances with whom they have some degree of familiarity and trust. The *Social zone* is the region surrounding the Personal zone, extending from approximately 1.2 to 3.6 m. This zone is typically used for more formal interactions, such as job interviews, and is generally considered an appropriate distance for strangers to interact. The *Public zone* is the region beyond the Social zone, extending beyond 3.6 m. This zone is used for public speaking and other formal interactions.

Early proxemics studies reported empirical results on zone sizes and utilities, but to use them for active interaction control in HRI, a generative, quantitative theory is needed. In the comprehensive review of proxemics for human–robot interactions proposed by Rios-Martinez et al. [5], it was suggested that 'quantitative models for shape, location and dynamics of personal space are interesting opportunities for collaborative research '.

CONTACT Fanta Camara fanta.camara@york.ac.uk

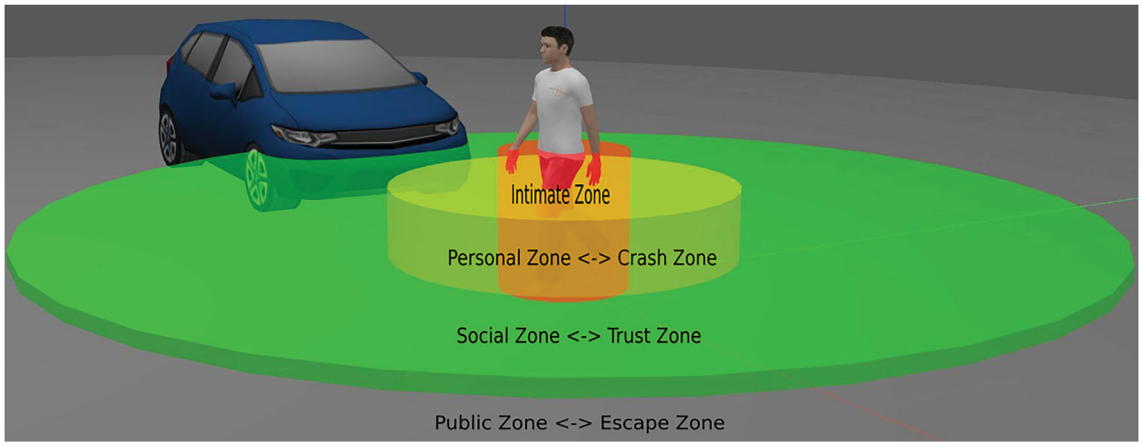

Figure 1. Vehicle entering pedestrian's social zone, which has been identified with the trust zone generated by the PTR model [4,6].

1.1. The PTR model

In [4], we proposed a generative, quantitative model of the Hall proxemics zones, called Physical Trust Requirement (PTR). From the perspective of some Agent_1, such as a pedestrian, vehicle or robot, states of the world including kinematics (position and velocity) of another Agent_2 can be classified as possessing PTR or not. PTR is present when Agent_1's future utility may be affected by an immediate decision to be made by Agent_2. Figure 1 shows the direct mapping between the PTR model and Hall's proxemics zones established in [4,6]. The set of locations of Agent_2 which give rise to PTR – for some choice of other parameters including both agents' sizes and speeds – was identified with Hall's social zone. The inner boundary of the social zone is called d_{crash} as if Agent_2 is within this boundary then a collision is certain to occur and neither agent can prevent it – even if they try to decelerate there is not enough time. The outer boundary is called d_{escape} because if Agent_2 is outside it then Agent_1 can always escape from a collision without depending on Agent_2. The social zone is the most interesting because here, Agent_1 has to rely on Agent_2. Agent_1 has no power to cause or prevent collision, but Agent_2 does have this power over Agent_1. This is an unpleasant situation for $Agent_1$, a negative utility.

We previously obtained analytical solutions for d_{escape} and d_{crash} for the case of a pedestrian crossing the road in front of, and orthogonal to, an oncoming car [4]. The zone sizes were found to depend on the size and speeds of both agents, and the braking ability of the car. We then found zone sizes for the case of two pedestrians interacting with one another, and for one pedestrian interacting with a humanoid robot [6]. This study also suggested that the two distances may vary as a function of the angle between Agent_1 and Agent_2. This suggestion was made using a simplified and unrealistic model that assumes Agent_1 can either turn on the spot or walk in a straight line. The study suggested that future work should consider more realistic strategies. This study thus considers such strategies, using numerical simulation to obtain approximate social zone shapes and sizes.

1.2. Contributions

The heading models in [6] assumed unrealistic dynamics in which Agent_1 first turns on the spot and then moves in a straight line, and suggested that future work should refine this assumption. The present study aims to do this by

- reviewing recent relevant empirical findings in the area of proxemics zones shapes and updating the PTR model based on these findings;
- solving the new model and finding new analytics solutions to reproduce some of the empirical observations for social zone outer boundary sizes and shapes in dual moving agents' interactions.

To our knowledge, this is the first kind of work deriving non-circular proxemics zone shapes and sizes from human kinematics. The results imply that robots interacting with humans should use non-circular proxemics zones to plan their interactions, and precise numerical sizes can be generated for use, which may vary between interactions depending on properties of the two agents. Such systems could be applied in robots including pavement delivery vehicles, self-driving cars, and humanoid assistive robots.

2. Empirical evidence for proxemics zone shapes

This section reviews recent relevant empirical findings in the area of proxemics zones shapes. Hall's theory defined

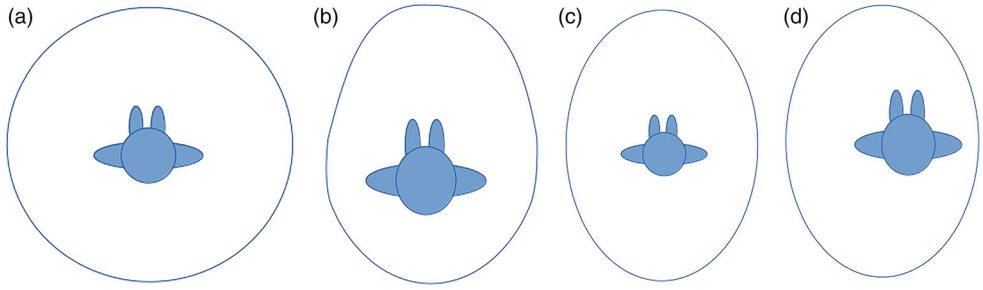

Figure 2. Types of proxemics zones shapes as reported by Rios-Martinez et al. [5]: (a) Circular, (b) Egg shape, (c) Elliptical, (d) Dominant side.

the four proxemics zones as concentric circles, and several empirical research works have used these commonly used circular proxemics zone shapes, cf. Figure 2(a). For example, Koay et al. [7] used the proxemics results from their previous studies that take into account the distance and approaching angle and showed that proxemics zones are of a circular shape. Aghaei et al. [8] developed a vision method to detect social distancing policy using a single image. In their work, the proxemics zones are represented as discs on the floor. However, Neef et al. have argued [9] that the inferred zone sizes and shapes can differ depending on the methods used for measurement.

Leichtmann et al. [10,11] have further critiqued the use of fixed zone sizes based on variations in additional social factors. For example, factors that affect human arousal levels or perceived situational control, such as room size or working memory load. They suggest the use of 'adaptive proxemics zone shapes' which dynamically respond to changes in these factors. Mumm and Mutlu [12] have studied physical and psychological distancing in human–robot interaction based on four existing theories of proxemic behaviour. Similarly, Bhagya et al. [13] developed an exploratory study on user proxemic preferences for interactions with robots that have different attributes, e.g. facial and vocal emotions and physical appearances. Samarakoon et al. [14] proposed a review on human–robot proxemics and in [15] the authors developed a proxemics-based approach method for a service robot that relies on the user physical behaviour and feedback. Walters et al. [16] proposed a framework that shows how to measure proxemic features in HRI. Their study involved participants interacting with different robots and their preferences were measured. It is explained that factors that may change human proxemics even by 20–150 mm can be significant.

Several recent studies have shown that proxemics zones are of non-circular shapes. For instance, Hayduk [17] investigated the 2D shape of personal space and found that egg-shaped zones describe best human proxemics zones, with a larger frontal space and smaller in the rear, and no difference found in preference in genders. Duncan and Murphy [18] reviewed 16 environmental and personal factors that affect proxemics distances in human–human and human–robot interactions, and based on which they introduced a model of comfortable distance. Ginés Clavero et al. [19] proposed adaptive proxemics zone shapes based on human activities, location, culture and specific situations. They adapted the asymmetric Gaussian function from Kirby et al. [20] and varied the parameters depending on activities such as cooking, running, standing and being in the bathroom. For example, an egg-shaped zone similar to Figure 2(b) was found for people that are moving.

In the social force model [21] often used to describe multiple agents interaction dynamics, personal space is part of the pedestrian's private sphere thus resulting into repulsive forces towards strangers to reduce uncomfortable situations. In this case, the proxemics zones can be modelled by concentric ellipses as suggested in [5] and shown in Figure 2(c). Patompak et al. [22] developed an inference method to learn human proxemics preferences. Their method is based on the social force model and reinforcement learning. They argued that proxemics spaces can be limited to two zones, the first being the quality interaction area where a robot could go without creating discomfort, and the private area which is the personal space. In addition, we believe that one more area is needed to model the trust relationship between humans and robots.

Lehmann et al. [23] measured human proxemics preferences with a small NAO robot with the assumption that the intimate zone is circular while the personal, social and public zones are elliptical. Jimenez et al. [24] proposed elliptic zone shapes for the interpersonal-social zone and the interpersonal-public zone used in a smart walker with social conventions. Kirks et al. [25] modelled and controlled interactions between workers and a socially interacting robot in a factory by using elliptical, worker-dependent proxemics zones in free navigation. Whilst [26] showed that proxemics zone shapes are asymmetrical during obstacle avoidance with some subjects tolerating a reduced personal space in their dominant

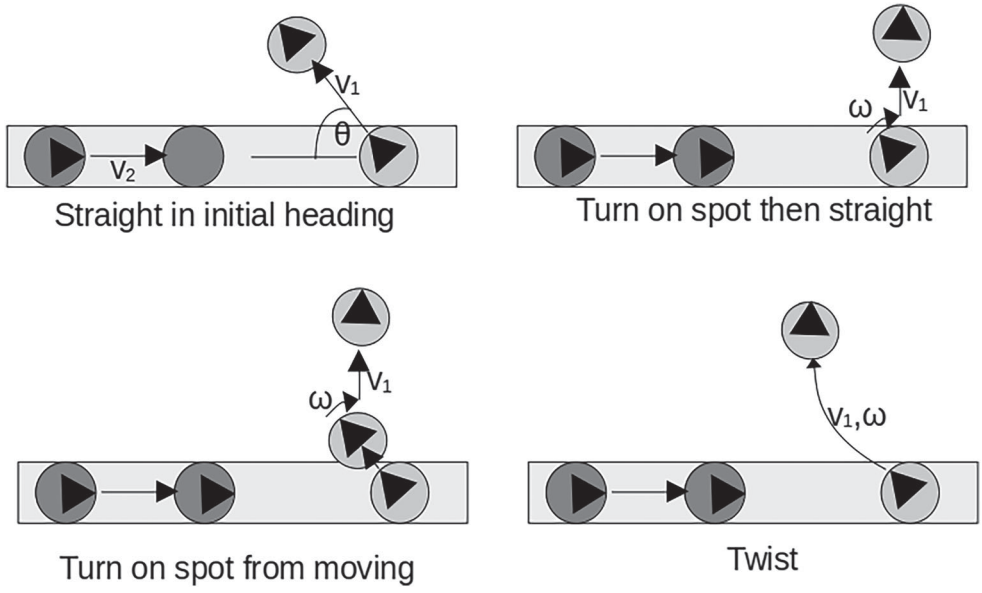

Figure 3. Geometries of the different strategies tested. In each strategy, $Agent_2$ is the darker circle, moving horizontally from left to right. $Agent_1$ is the lighter circle.

side, as shown in Figure 2(d). Neggers et al. [27] showed that 'experimental research on how robots can avoid a person in a comfortable way is largely missing'. Their empirical findings suggest that the outer proxemics zone shape is not circular and that passing at the back of a person is more uncomfortable compared to passing at the front. Their results showed an empirical 'comfort' zone, probably inverse of hall zones, which match the elliptical shapes expected.

The proxemics zone shapes shown in Figure 2 summarize these findings which support the idea of non-circular zones to best describe human proxemics.

3. Methods

3.1. Assumptions

We here derive analytical equations and their visual shapes for the outer boundary of the social zone (d_{escape}) for a human $Agent_1$ being approached by another human or robot, $Agent_2$, using the PTR model [4,6]. We assume that $Agent_2$ travels in a straight line towards $Agent_1$ and does not turn or brake to avoid collision.

Both agents are assumed to be circular with width (diameter) w. The agents could be humans, humanoid robots, or vehicles. The strategies examined are chosen to be amenable to exact or approximate analytic solutions while representing plausible though simplified kinematics of both human and wheeled agents. To simplify the equations, we approximate all models by assuming that the minimal collision occurs exactly when $Agent_1$ has left the collision corridor. We assume the same values for the kinematic parameters across the strategies.

Unlike previous work, we will now take account of the initial heading of $Agent_1$ relative to the direction of approach by $Agent_2$, and of various possible strategies that $Agent_1$ could use to optimise their escape distance in order to reduce the zone sizes.

As in [6], we provide numerical results for two cases: human–human interaction (HHI) and human–robot interaction (HRI) where we assume that a human walker is interacting with a humanoid robot such as PR2. These values for human pedestrians were obtained from the empirical literature and used in our previous study [6] and are: speed $v = 1.1$ m/s, width $w = 1.19$ m, thinking or reaction time $t = 1.1$ s, turning speed $\omega = 1.0$ rad/s. The values for HRI were similarly obtained from realistic robot estimates in the previous paper [6] and are: $t_1 = 1.1$ s, $t_2 = 0.5$ s, $v_1 = 1.1$ m/s, $v_2 = 1.0$ m/s, $w_1 = 1.19$, $w_2 = 0.4$ m with index 1 for the human and 2 for the robot.

3.2. Strategies

The strategies are illustrated in Figure 3. $Agent_1$ begins the scenario oriented at angle θ from the approach of $Agent_2$. $Agent_1$ then attempts to avoid collision by escaping from the collision corridor formed by $Agent_2$'s path, using its maximum linear speed v_1 and maximum angular velocity ω in different ways as explained and solved in the following subsections.

3.2.1. Baseline strategy: instant turn on spot

As a baseline, the first experiment reproduces previous results of Option 1 in [6], but presenting them in a new

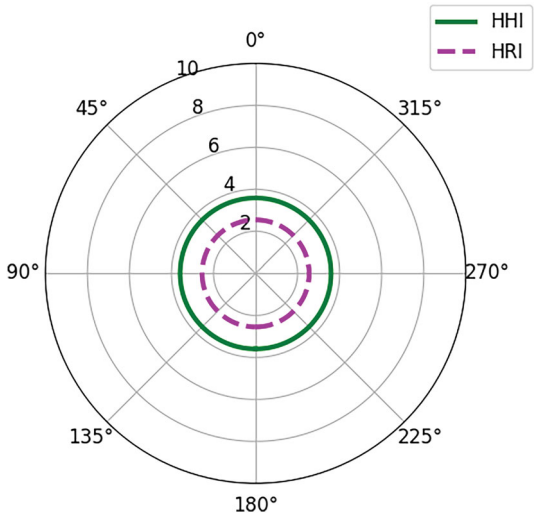

Figure 4. Instant turn on spot.

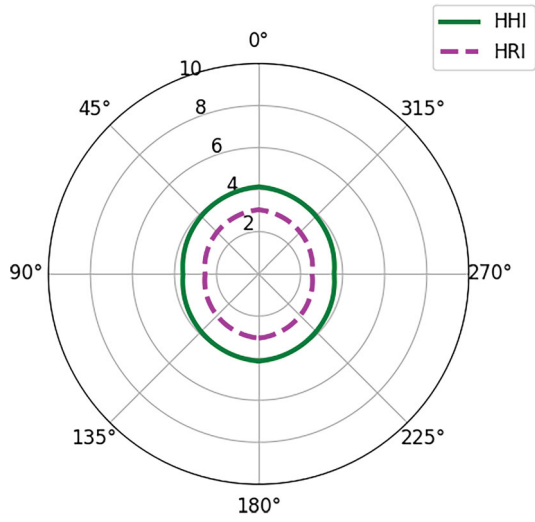

Figure 5. Turn on the spot then straight.

polar form. This strategy assumes that Agent_1 may turn on the spot to any heading instantaneously, then move forwards in a straight line. Regardless of initial heading, the optimal strategy is thus always to rotate to face orthogonally to Agent_2, then walk straight forwards to escape.

The analytic solution was found in [6] to be

$$d_{escape} = v_2 t_1 + (w_1 + w_2)\frac{v_2}{v_1}, \tag{1}$$

where $w_1 + w_2$ is the total distance that Agent_1 must travel in front of Agent_2 to avoid contact with Agent_2. The resulting zone shape is a perfect circle, as shown in Figure 4 because the initial turn on the spot takes no time and escapes from all initial headings then follows the same straight trajectory.

3.2.2. Strategy: straight in initial heading

In this strategy, Agent_1 tries to escape by moving forward in a straight line in the direction of their initial heading, they do not rotate at all. The analytical solution [6] was previously found to be

$$d_{escape} = v_2 t_1 + (w_1 + w_2)\frac{v_2}{v_1|\sin(\theta)|}. \tag{2}$$

It was plotted there as a U-shaped Cartesian graph. To enable comparison with the other new strategies, it is now plotted in polar coordinates because this shows the actual physical shape of the zones. The resulting zone is shown in Figure 8(a).

3.2.3. Strategy: turn on spot then straight

This strategy was previously suggested as future work in [6] and is tested here for the first time analytically. In this option, Agent_1 begins standing stationary at angle θ to Agent_2's heading. Agent_1 first turns on the spot at angular velocity ω, until they are orthogonal to the other's approach, and then moves forward at speed v_1. The rotation direction is chosen to be the shortest to reach the orthogonal direction, so that,

$$d_{escape} = v_2 t_1 + (w_1 + w_2)\frac{v_2}{v_1} + v_2(|\pi/2 - |\theta||)/\omega. \tag{3}$$

Here we are assuming that it is always best to take time to rotate to 90 degrees first. This seems sensible for normal humans, but we could imagine mathematical cases where the rotate speed is very slow relative to forward speed, where it might be more optimal to rotate to some smaller angle. We are assuming that turning on the spot is 'fast' compared to walking forwards. The analytical solution is shown in Figure 5.

3.2.4. Strategy: turn on spot from moving

This strategy was also suggested as future work [6] and is tested for the first time here. In this model, Agent_1 begins moving in their heading direction and continues to do so during their thinking time, as in Straight In Initial Heading. Then Agent_1 stops instantly and behaves as in Turn on the Spot then Straight.

During their thinking time, Agent_1 travels $v_1 t_1 \sin(\theta)$ vertically and $d_1 = v_1 t_1 \cos(\theta)$ horizontally (which may be positive or negative). This vertical distance travelled reduces the remaining vertical distance needed to escape the collision corridor to $w_1/2 + w_2 - v_1 t_1 \sin(\theta)$. The turning time is the same as in the turn then straight strategy, $(|\pi/2 - |\theta||)/\omega$.

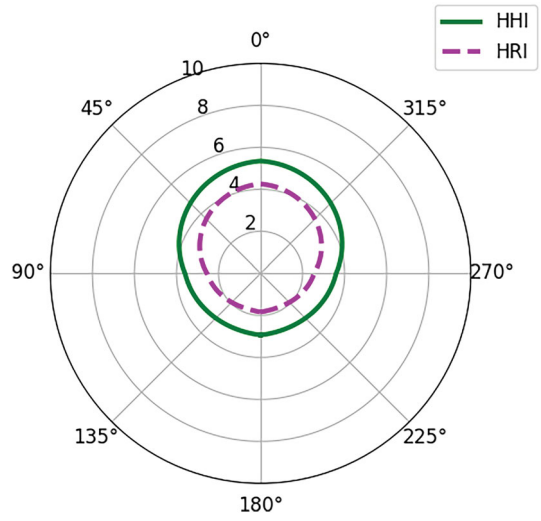

Figure 6. Turn on the spot from moving.

The total escape time is thus

$$\tau = t_1 + (|\pi/2 - |\theta||)/\omega + (w_1/2 + w_2/2 - v_1 t_1 \sin(\theta).)/v_1 \quad (4)$$

Agent_2 will travel at v_2 during this time, giving escape distance,

$$d_{escape} = v_2(t_1 + (|\pi/2 - |\theta||)/\omega + (w_1/2 + w_2/2 - v_1 t_1 \sin(\theta))/v_1). \quad (5)$$

The resulting zone boundary is shown in Figure 6.

3.2.5. Strategy: twist

This is a new strategy, which assumes that Agent_1 can and does turn during forward travel, where turning takes place at angular velocity ω at the same time as moving with forward velocity v_1. Twists produce arc segments of motion, around a 'great circle' whose radius is given by $r = v/\omega$. Both v and ω are properties of Agent_1, describing how fast they can move forwards and turn. This strategy assumes that the direction (clockwise or anticlockwise) of the twist is chosen as the one which is closest to orthogonal to Agent_2's approach.

Figure 7 shows the assumed geometry of the twist strategy, annotated with the angles and lengths which will be used in the derivation. Unlike the other strategies, we will here assume that the robot in the HRI case has the same width w as the pedestrian, to simplify the geometry.

Agent_1 is trying to escape from Agent_2 by moving in a Twist, around the great circle of radius $r = v/\omega$. Agent_2 is approaching from left to right at speed v_2. Call the area swept out by Agent_2 the 'collision corridor'. The collision corridor is shown as the very light grey rectangle in the figure. Agent_1's poses are shown in Figure 7 as two light grey circles. Agent_2 poses are shown as two dark grey circles. Agent_1's start pose is labelled A1S and their end pose, just out of the collision corridor, as A1E. Agent_2's start pose is labelled A2S, and a possible end pose, at which a collision is just averted, is labelled A2E. Define the distance between A2S and A2E as the escape distance, d_{escape}. Agent_1 begins the scenario facing in direction x', at angle θ clockwise from the approach of Agent_2. θ thus

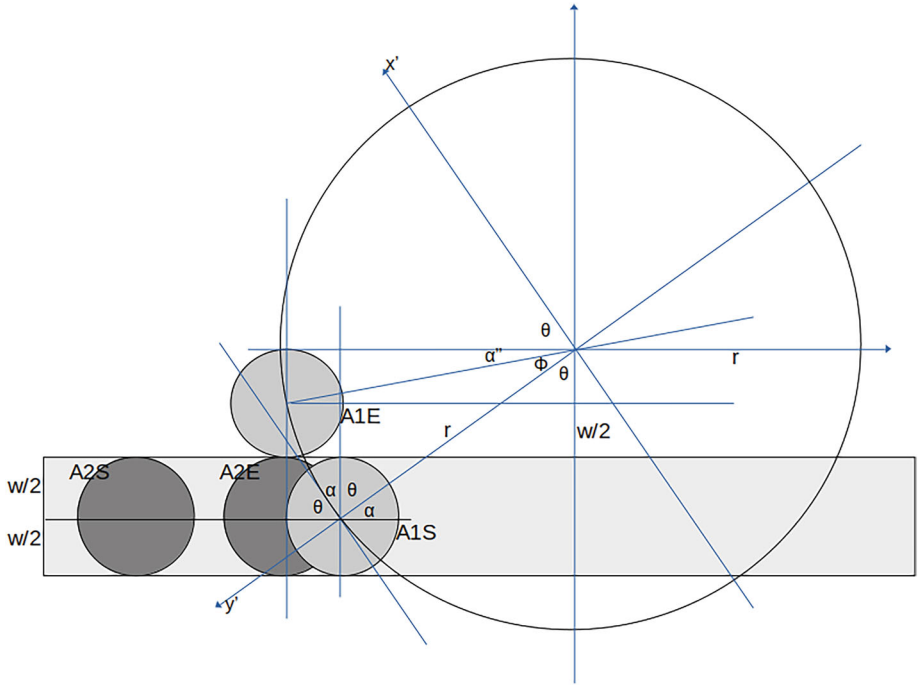

Figure 7. Twist strategy geometry.

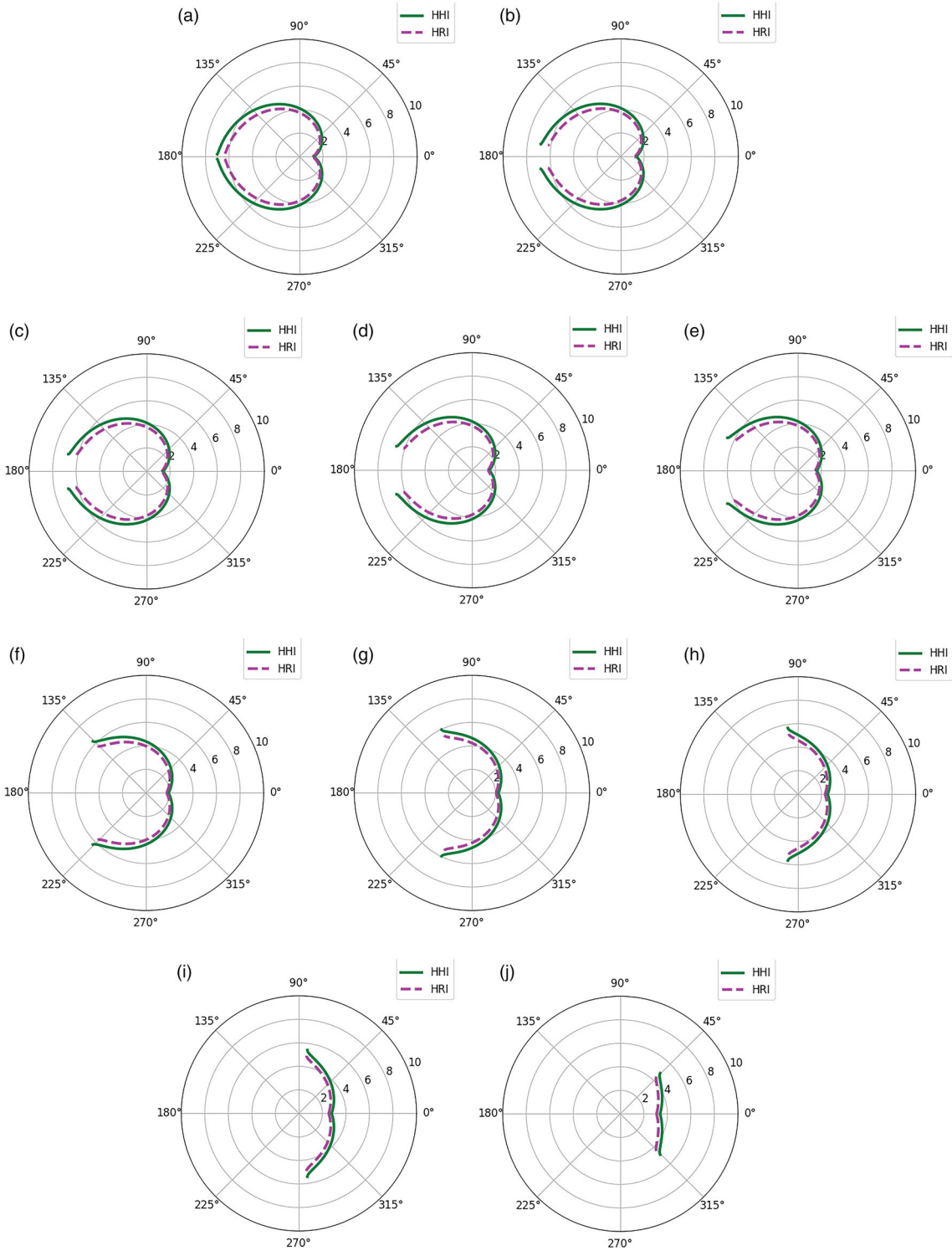

Figure 8. Twist model using different values of turning speed ω. Note that $\omega = 0$ is a special case of linear motion, which is the Straight in Initial Heading strategy: (a) $\omega = 0.0$ deg/s, (b) $\omega = 0.625$ deg/s, (c) $\omega = 1.25$ deg/s, (d) $\omega = 2.5$ deg/s, (e) $\omega = 5$ deg/s, (f) $\omega = 15$ deg/s, (g) $\omega = 30$ deg/s, (h) $\omega = 45$ deg/s, (i) $\omega = 60$ deg/s, (j) $\omega = 90$ deg/s.

defines the tangent angle of the great circle at A1S. This tangent and the radius r fully define the great circle.

Define the complement of θ,

$$\alpha = \frac{\pi}{2} + \theta. \tag{6}$$

Define the angle around the great circle which Agent_1 needs to travel to leave the collision corridor as ϕ.

Define the complement of $(\theta + \phi)$ as

$$\alpha'' = \frac{\pi}{2} - (\phi - \theta), \tag{7}$$

because Agent_1 is moving with an angle θ but in the clockwise direction.

From the geometry of the figure,

$$r \sin \alpha'' = r \cos \theta - w. \tag{8}$$

Rearranging this gives

$$\alpha'' = \sin^{-1}\left(\cos\theta - \frac{w}{r}\right). \tag{9}$$

Substituting the left-hand side

$$\pi/2 - \phi + \theta = \sin^{-1}\left(\cos\theta - \frac{w}{r}\right). \tag{10}$$

Rearranging, we can now solve for ϕ,

$$\phi = \frac{\pi}{2} - \sin^{-1}\left(\cos\theta - \frac{w}{r}\right) + \theta. \tag{11}$$

The time taken for Agent_1 to move around the great circle from A1S to A1E is ϕ/ω. During the sum of these times, Agent_2 travels towards Agent_1 at speed v_2. So the starting distance between them, d_{escape}, which results in just avoiding collision, and thus forms the outer boundary of the social zone is given by

$$d_{escape} = v_2 t_1 + v_2 \frac{\phi}{\omega}. \tag{12}$$

ϕ has a solution if

$$-1 \leqslant \cos\theta - \frac{w_1}{r} \leqslant 1 \tag{13}$$

That gives

$$\arccos\left(\frac{w_1}{r} + 1\right) \leqslant \theta \leqslant \arccos\left(\frac{w_1}{r} - 1\right). \tag{14}$$

Then we have

$$\frac{w_1}{r} - 1 \geqslant -1 \quad \text{and} \quad \frac{w_1}{r} - 1 \leqslant 1 \tag{15}$$

$$\frac{w_1}{r} \geqslant 0 \quad \text{and} \quad \frac{w_1}{r} \leqslant 2 \tag{16}$$

$$\frac{w_1}{r} \geqslant 0 \quad \text{and} \quad r \geqslant \frac{w_1}{2} \tag{17}$$

The results of these equations for the Twist strategy are shown in Figure 8 from the perspective of Agent_1 facing Agent_2 at 180 degrees. If ω is very fast (relative to v_2), then it will behave like Strategy Turn on the Spot. If ω is very slow (relative to v_2), then it will behave like Strategy Straight Line in Initial Heading Direction. Those two previous strategies are thus special and limiting cases of the general twists, as was suggested in [6].

4. Discussion

The results show that the human proxemics zones generated by kinematics under the PTR model become non-circular due to changes in the time required for the human to escape from impending collisions. The outer boundary of the social zone retains its usual assumed value of 3.6 m when two human agents begin at right angles, but becomes larger towards the front of the person and smaller behind them. The precise shape depends on details of what strategy model is assumed for the pedestrian kinematics.

This is the first time that non-circular proxemics has been generatively and quantitatively modelled from human kinematic behaviour to explain the deformation of Hall's zones as a function of rotation and motion of the agents. Non-circular zones have previously been observed empirically, as shown in Figure 2 but not explained. For example, Kirby's model [20] and some others assumed quantitative non-circular zones to fit these empirical results, but did not derive them from generative kinematics. The HRI zone boundaries are generally smaller than the HHI ones, this is consistent with previous empirical studies. This is because the robot is smaller and slower than a human, so poses less of a threat to the human whom it is approaching. The human is therefore willing for it to come closer than another human.

Some of the twist cases produce no solution for d_{escape}, which can be seen by the absence of complete paths around the 360 degrees in Figure 8. This may be due to the analytical equation being derived from the geometric arguments of Figure 7. This figure uses standard geometric reasoning to propagate angles across the constructions. But it is drawn for a particular value of θ so it is possible that cases may exist where these arguments are not valid, and which result in the loss of solutions or in which the solutions exist but are inaccurate. These might correspond to real cases in which the twist strategy is not useful, in which real pedestrians would switch to some other behaviour in its place. For example, if ω is very large compared to v_1, the twist strategy would result in the agent spinning around in a small circle contained entirely within the collision corridor and never escaping. Future work could investigate these cases using more detailed kinematic models, and how real pedestrians change between strategies. It could also consider twists in HRI cases where the agents have different widths.

Future work should also extend the model to derive the inner boundary of the social zone, formed when Agent_2 acts to try to prevent the collision by braking. There have been recent empirical observations [28,29],

which suggest that zone boundaries stretch as functions of both agents' initial speeds, including to long (tens of meters) ranges when dealing with high-speed vehicles – which may be related to the stopping distances taught to and used by human drivers. The current model could be used to explore these effects to see if they match with these stopping distances. The resulting zone shapes could be compared with and calibrated to a more detailed review of known empirical zones in different settings.

The model proposed in this work is based only on kinematics so is not able to explain the adaptive proxemics zone shapes of [10,11] reviewed above. These changes are hypothesized to be caused by additional social factors such as attention and perceived control. Our current model assumes that the agents have perfect information and computation resources. Real humans are constrained by noisy, uncertain information and, restricted computation, and various utilities and biases which might be added to the model in the future to capture these social effects.

Acknowledgments

The authors would like to thank the associate editor and the reviewers for their feedback to help improve the quality of this paper.

Disclosure statement

No potential conflict of interest was reported by the author(s).

Funding

This work has received funding from the EU H2020 project interACT: Designing cooperative interaction of automated vehicles with other road users in mixed traffic environments under grant agreement no. 723395.

Notes on contributors

Fanta Camara is a research fellow at the Institute for Safe Autonomy, University of York, UK. She completed her PhD at the Institute for Transport Studies (ITS), University of Leeds, UK. She was a postdoctoral researcher and visiting researcher at the Lincoln Centre for Autonomous Systems (LCAS) in the School of Computer Science, University of Lincoln, UK. She obtained her Master degree in robotics engineering from Sorbonne University (former Université Pierre et Marie Curie, UPMC), Paris, France, and she was an exchange student at National Taiwan University, Taipei, Taiwan. Her PhD thesis won the second place at the Queen Mary UK Best PhD in Robotics Award 2022 and she also won the UK Robotics and Autonomous Systems (UK-RAS) Network Rising Star Award 2022.

Charles Fox obtained an MA in computer science at the University of Cambridge, MSc in cognitive science at the University of Edinburgh, and his DPhil in engineering from the Robotics Research Group at the University of Oxford. He worked as a data-driven high-frequency hedge fund trader in London then as a researcher at the Sheffield Center for Robotics and as an autonomous vehicle fellow at the Institute for Transport Studies, University of Leeds. He is currently a senior lecturer in robotics and autonomous systems at the University of Lincoln, UK.

References

[1] Trautman P, Krause A. Unfreezing the robot: navigation in dense, interacting crowds. In: Proceedings of the IEEE/RSJ International Conference on Intelligent Robots and Systems (IROS); 2010. p. 797–803. doi:10.1109/IROS.2010.5654369

[2] Fox CW, Camara F, Markkula G, et al. When should the chicken cross the road? game theory for autonomous vehicle – human interactions. In: VEHITS: 4th International Conference on Vehicle Technology and Intelligent Transport Systems; 2018 Jan. doi:10.5220/0006765404310439

[3] Hall ET. The hidden dimension. Vol. 609. Garden City (NY): Doubleday; 1966.

[4] Camara F, Fox C. Space invaders: pedestrian proxemic utility functions and trust zones for autonomous vehicle interactions. Int J Soc Robot. 2020; doi:10.1007/s12369-020-00717-x

[5] Rios-Martinez J, Spalanzani A, Laugier C. From proxemics theory to socially-aware navigation: a survey. Int J Soc Robot. 2015;7(2):137–153. doi:10.1007/s12369-014-0251-1

[6] Camara F, Fox C. Extending quantitative proxemics and trust to HRI. In: Proceedings of the 31st IEEE International Conference on Robot & Human Interactive Communication (RO-MAN); 2022. (Best Student Award Paper Finalist and KROS Interdisciplinary Research Award in Social Human–Robot Interaction Finalist). doi:10.1109/RO-MAN53752.2022.9900821

[7] Koay KL, Syrdal D, Bormann R, et al. Initial design, implementation and technical evaluation of a context-aware proxemics planner for a social robot. In: Social Robotics: 9th International Conference, ICSR 2017, Tsukuba, Japan, November 22–24, 2017, Proceedings 9. Springer; 2017. p. 12–22. doi:10.1007/978-3-319-70022-9_2

[8] Aghaei M, Bustreo M, Wang Y, et al. Single image human proxemics estimation for visual social distancing. In: Proceedings of the IEEE/CVF Winter Conference on Applications of Computer Vision; 2021. p. 2785–2795.

[9] Neef NE, Zabel S, Lauckner M, et al. What is appropriate? on the assessment of human–robot proxemics for casual encounters in closed environments. Int J Soc Robot. 2023:1–15. doi:10.1007/s12369-023-01004-1

[10] Leichtmann B, Lottermoser A, Berger J, et al. Personal space in human–robot interaction at work: effect of room size and working memory load. ACM Trans Hum Robot Interact (THRI). 2022;11(4):1–19. doi:10.1145/3536167

[11] Leichtmann B, Nitsch V. How much distance do humans keep toward robots? literature review, meta-analysis, and theoretical considerations on personal space in human–robot interaction. J Environ Psychol. 2020;68:101–386. doi:10.1016/j.jenvp.2019.101386

[12] Mumm J, Mutlu B. Human–robot proxemics: physical and psychological distancing in human–robot interaction. In: Proceedings of the 6th International Conference on Human–Robot Interaction; 2011. p. 331–338. doi:10.1145/1957656.1957786

[13] Bhagya S, Samarakoon P, MA V, et al. An exploratory study on proxemics preferences of humans in accordance with attributes of service robots. In: 28th IEEE International Conference on Robot and Human Interactive Communication (RO-MAN); 2019. p. 1–7. doi:10.1109/RO-MAN46459.2019.8956297

[14] Samarakoon BP, Muthugala MVJ, Jayasekara ABP. A review on human–robot proxemics. Electronics. 2022;11(16):2490. doi:10.3390/electronics11162490

[15] Samarakoon SBP, Muthugala MVJ, Jayasekara ABP, et al. Adapting approaching proxemics of a service robot based on physical user behavior and user feedback. User Model User Adapt Interact. 2023;33(2):195–220. doi:10.1007/s11257-022-09329-8

[16] Walters ML, Dautenhahn K, Te Boekhorst R, et al. An empirical framework for human–robot proxemics. Proc New Front Hum Robot Interact. 2009. Available from: http://hdl.handle.net/2299/9670

[17] Hayduk LA. The shape of personal space: an experimental investigation. Can J Behav Sci. 1981;13(1):87. doi:10.1037/h0081114

[18] Duncan BA, Murphy RR. A preliminary model for comfortable approach distance based on environmental conditions and personal factors. In: IEEE International Conference on Collaboration Technologies and Systems (CTS); 2012. p. 622–627. doi:10.1109/CTS.2012.6261117

[19] Ginés Clavero J, Martín Rico F, Rodríguez-Lera FJ, et al. Defining adaptive proxemic zones for activity-aware navigation. In: Advances in Physical Agents II: Proceedings of the 21st International Workshop of Physical Agents (WAF 2020), November 19–20, 2020, Alcalá de Henares, Madrid, Spain. Springer; 2021. p. 3–17. doi:10.1007/978-3-030-62579-5_1

[20] Kirby R, Simmons R, Forlizzi J. Companion: a constraint-optimizing method for person-acceptable navigation. In: International Symposium on Robot and Human Interactive Communication (RO-MAN); 2009. p. 607–612. doi:10.1109/ROMAN.2009.5326271

[21] Helbing D, Molnar P. Social force model for pedestrian dynamics. Phys Rev E. 1995;51(5):4282. doi:10.1103/PhysRevE.51.4282

[22] Patompak P, Jeong S, Nilkhamhang I, et al. Learning proxemics for personalized human–robot social interaction. Int J Soc Robot. 2019:1–14. doi:10.1007/s12369-019-00560-9

[23] Lehmann H, Rojik A, Hoffmann M. Should a small robot have a small personal space? investigating personal spatial zones and proxemic behavior in human–robot interaction. 2020. Available from: arXiv preprint arXiv:2009.01818.

[24] Jiménez MF, Scheidegger W, Mello RC, et al. Bringing proxemics to walker-assisted gait: using admittance control with spatial modulation to navigate in confined spaces. Pers Ubiquitous Comput. 2022;26(6):1491–1509. doi:10.1007/s00779-021-01521-8

[25] Kirks T, Jost J, Finke J, et al. Modelling proxemics for human–technology-interaction in decentralized social-robot-systems. In: Ahram T, Karwowski W, Vergnano A, et al., editors. Intelligent human systems integration 2020. Cham: Springer International Publishing; 2020. p. 153–158. doi:10.1007/978-3-030-39512-4_24

[26] Gérin-Lajoie M, Richards CL, Fung J, et al. Characteristics of personal space during obstacle circumvention in physical and virtual environments. Gait Posture. 2008;27(2):239–247. doi:10.1016/j.gaitpost.2007.03.015

[27] Neggers MM, Cuijpers RH, Ruijten PA, et al. Determining shape and size of personal space of a human when passed by a robot. Int J Soc Robot. 2022:1–12. doi:10.1007/s12369-021-00805-6

[28] Neef N, Kastner K, Schmidt M, et al. On optimizing driving patterns of autonomous cargo bikes as a function of distance and speed – a psychological study. IEEE Open J Intell Transp Syst. 2022;3:592–601. doi:10.1109/OJITS.2022.3198120

[29] Neggers MME, Cuijpers RH, Ruijten PAM, et al. The effect of robot speed on comfortable passing distances. Front Robot AI. 2022;9. doi:10.3389/frobt.2022.915972